JOURNAL OF BACTERIOLOGY, Oct. 1992, p. 6460–6470
0021-9193/92/206460-11$02.00/0

Vol. 174, No. 20

Detection of Growth Sites in and Protomer Pools for the Sheath of *Methanospirillum hungatei* GP1 by Use of Constituent Organosulfur and Immunogold Labeling

G. SOUTHAM* AND T. J. BEVERIDGE

Department of Microbiology, College of Biological Science, University of Guelph, Guelph, Ontario, Canada N1G 2W1

Received 17 January 1992/Accepted 30 July 1992

***Methanospirillum hungatei* GP1 integrated approximately 9% of cellular [^{35}S]cysteine into its sheath. Autoradiography of sodium dodecyl sulfate-polyacrylamide gels revealed that [^{35}S]cysteine was confined to the proteins released by the sodium dodecyl sulfate–β-mercaptoethanol–EDTA solubilization method (G. Southam and T. J. Beveridge, J. Bacteriol. 173:6213–6222, 1991) and was not present in the proteins released by treatment with phenol (G. Southam and T. J. Beveridge, J. Bacteriol. 174:935–946, 1992). Limited labeling of exposed sulfhydryl groups on hoops produced from sheath material suggested that most organosulfur groups occur within hoops and therefore help contribute to resilience. Electron microscopic autoradiography demonstrated that sheath growth, which is most active at the sites of cell division (spacer region), occurs through the de novo development of hoops. For growth to occur in the spacer region, sheath precursors must transverse several periodic envelope layers, including the cell wall (a single layer) and the various lamellae of the spacer plug (T. J. Beveridge, G. D. Sprott, and P. Whippey, J. Bacteriol. 173:130–140, 1991).**

For many eubacteria and archaeobacteria, surface arrays (S layers) represent the outer interface between the cell and its environment. Although the function(s) of S layers is not always readily apparent, it is likely that they serve a protective role by modulating deleterious environmental effects on the underlying cell.

The proteinaceous sheath of *Methanospirillum hungatei* GP1 is an unusual bacterial S layer owing to its persistent stability in the presence of typical ionic (chaotropic) and nonionic detergents, denaturants, and degradative enzymes (6). Functionally, the sheath possesses an exquisite sieving character, allowing the penetration of molecules only as large as acetate into the cells (5). Most bacterial S layers do not possess intersubunit covalent bonding; however, the sheath of *M. hungatei* appears to be an exception. The sheath, which exhibits resilience to all other chemical perturbants, is partially solubilized after exposure to the disulfide bond-breaking agent β-mercaptoethanol (β-ME [25]), which chemically reduces cystine to two cysteines. In that study (25), the sheath cylinder was split into constituent hoops (likened to barrel hoops so that one can imagine a sheath to be an assemblage of hoops with each hoop sequentially on top of the other to form a tube). Despite the very low levels (0.62 mol%) of cysteine previously detected by amino acid analysis of the sheath (6, 18) and the fact that most S layers are devoid of cysteine (21), it seems plausible that the strategic location of disulfide bonds could contribute to the stability of the sheath.

The localization of this sulfur to specific sheath polypeptides (22, 23) was essential for the development of a model for the sheath structure and for understanding the resilience of the sheath. This study examined purified sheath (6) and hoops (25) for the occurrence of total sulfur and surface-exposed sulfhydryl groups, respectively. As *M. hungatei* was capable of utilizing cysteine as an organosulfur source (15), [^{35}S]cysteine provided a means for studying cell growth through its incorporation into the sheath. Finally, monoclonal antibodies (MAbs) specific for the sheath polypeptides were used to localize pools of sheath precursors within the bacterium.

MATERIALS AND METHODS

Bacterial growth conditions. *M. hungatei* GP1 (17) was grown in 1-liter culture bottles modified to accept 22-mm butyl rubber stoppers and aluminum seals (Pegasus Industries Ltd., Scarborough, Ontario, Canada). These culture vessels contained 100 ml of SA medium (16) and were gassed daily with an H_2-CO_2 (80:20) mixture. For most experiments, the bacterium was grown to an optical density at 600 nm (path length, 1 cm) of 0.500 to 1.00, which represents a mid-exponential to early stationary growth phase. All chemicals used in this study were from Fisher Scientific Co., Fair Lawn, N.J., unless otherwise stated.

Transmission electron microscopy. Standard embedding of *M. hungatei* and negative staining of cells or component parts have been described (22).

M. hungatei was also embedded in Lowicryl K4M resin (Marivac, Halifax, Nova Scotia, Canada) to aid antibody localization. A 1-ml culture aliquot of *M. hungatei* was fixed in 1% aqueous glutaraldehyde for 2 h at 4°C. The cells were pelleted by centrifugation at 14,000 × *g* for 30 s with an Eppendorf microcentrifuge (Brinkmann, Rexdale, Ontario, Canada) and washed once with distilled H_2O (dH_2O). The cells were enrobed in 2% (wt/vol) Noble agar, cut into small blocks, transferred to 25% (vol/vol) ethanol at 0°C, and incubated for 30 min. The blocks were then processed through the following ethanol dehydration series with 1-h incubations at −20°C: 50% (vol/vol), 80% (vol/vol), 95% (vol/vol), and 100% ethanol. The following embedding procedure also was done at −20°C. Blocks were transferred to Lowicryl K4M resin-ethanol (1:1) for 1 h. Further transfers included resin-ethanol (2:1) and pure resin, both for 1 h.

* Corresponding author.

TABLE 1. Distribution of ^{35}S in *M. hungatei* during purification of the sheath

Sample or step	Distribution of ^{35}S (dpm/ml) at day:	
	14	28
Total label in the culture system[a]	12,150,370 ± 289,023 (5.65)	5,278,320 ± 10,592 (12.17)
Cellular label[b]	698,057 ± 28,344 (100.0)	642,367 ± 3,347 (100.0)
NaOH extraction (removes spacer plugs)[b]	654,591 ± 11,588 (84.36)	563,524 ± 17,169 (83.19)
SDS extraction (removes membrane and cytoplasmic debris)[b]	49,966 ± 4,378 (7.16)	47,840 ± 3,421 (7.45)
Purified sheath[b]	59,194 ± 679 (8.48)	60,132 ± 2,561 (9.36)

[a] Numbers in parentheses represent the percentage of experimental label that was cellular.
[b] Numbers in parentheses represent the percentage of incorporation relative to total cellular incorporation.

Infiltration was continued in pure resin overnight. On the following day, the blocks were transferred to pure resin for a further 4 h of incubation and then embedded in a gelatin capsule containing additional pure resin. Polymerization was initiated by illuminating the blocks with a 366-nm UV light (model UVL-21; Blak-Ray, San Gabriel, Calif.) at −20°C for 48 h and then at room temperature for 24 h. The embedded blocks were kept at room temperature for a further 48 h with no UV light and were then stored with dessicant at 4°C until use.

Cellular [^{35}S]cysteine incorporation. To determine the importance of sulfur proteins and their disulfide bonds in the sheath, we inoculated actively growing 100-ml cultures of *M. hungatei* with 40 μl of [^{35}S]cysteine (with a specific activity of 1 mCi/100 μl; Amersham Ltd., Oakville, Ontario, Canada) to specifically label these proteins. The culture bottles were gassed daily as described above. Samples were taken on days 1, 14, and 28 to determine, by liquid scintillation counting, the level of [^{35}S]cysteine incorporation. Owing to the large amount of label used, the growth of *M. hungatei* was not monitored as the optical density at 600 nm.

Detection of the ^{35}S label in the sheath. On both days 14 and 28 (after the addition of [^{35}S]cysteine to the culture medium), the ^{35}S-labeled cultures of *M. hungatei* were processed to purify the sheath structures. These cultures were harvested by centrifugation (14,000 × *g*). To determine the level of incorporation of ^{35}S, we placed aliquots of cells from 1 ml of culture and 1 ml of culture supernatant into scintillation vials for counting. In addition, aliquots of all treatments and washes obtained during sheath purification were placed into scintillation vials for counting. The ^{35}S-labeled *M. hungatei* cells (see above) were treated as follows. The cell pellet was resuspended in 10 ml of 0.1 N NaOH and incubated, with mixing, at room temperature for 1 h to lyse the cells and facilitate their removal from the sheath. This preparation was centrifuged as described above; the supernatant was removed and the pellet was resuspended in 10 ml of dH_2O. This crude sheath preparation was washed four times with 10 ml of dH_2O. The pellet containing the crude sheath was resuspended in 10 ml of 1% (wt/vol) sodium dodecyl sulfate (SDS) and incubated at 100°C for 1 h with occasional mixing to remove adsorbed membrane from the sheath. This reaction mixture was centrifuged, and the sheath pellet was washed four times with dH_2O to ensure the removal of any solubilized components and remaining SDS. All of the treatments and washes were examined for the presence of ^{35}S. Each of the samples for scintillation counting received 1 ml of Protosol (New England Nuclear, Mississauga, Ontario, Canada) to solubilize bacterial cells or their components and 10 ml of Scintiverse I to facilitate scintillation counting in an aqueous system. Counting for the presence of ^{35}S was done with a liquid scintillation analyzer from Packard Scientific, Downers Grove, Ill.

SDS-PAGE and autoradiography. ^{35}S-labeled sheath samples (75 μg [dry weight]) were solubilized with SDS–β-ME–EDTA treatment for 2 h (22). The labeled sheath was also fractionated as phenol-soluble (PS) and phenol-insoluble (PI) preparations (23) as follows. Intact sheath was treated with 90% (wt/vol) phenol overnight at room temperature. This reaction mixture was centrifuged at 175,000 × *g* for 1 h, and the supernatant (PS) and pellet (PI) were dialyzed against 2% (wt/vol) SDS prior to further analysis. These samples were separated by SDS-polyacrylamide gel electrophoresis (PAGE) (12) and stained with Coomassie brilliant blue R-250, and the gel was dried in a gel dryer (Bio-Rad, Richmond, Calif.). The dried gel was exposed to X-Omat AR X-ray film (Eastman Kodak Co., Rochester, N.Y.) for up to 1 week. The autoradiographic film was developed for 2 min in D19 (Eastman Kodak), development was stopped with 2% (vol/vol) acetic acid (1 min), and the film was fixed for 5 min in Rapid Fixer (Eastman Kodak) before being washed with dH_2O (30 min).

Electron microscopic autoradiography (EM autoradiography). Both day-14 and day-28 ^{35}S-labeled sheath samples were applied to Formvar carbon-coated grids. Ilford L-5 autoradiographic emulsion gel was maintained in a liquid form with a 60°C water bath. With a wire loop, a thin film of

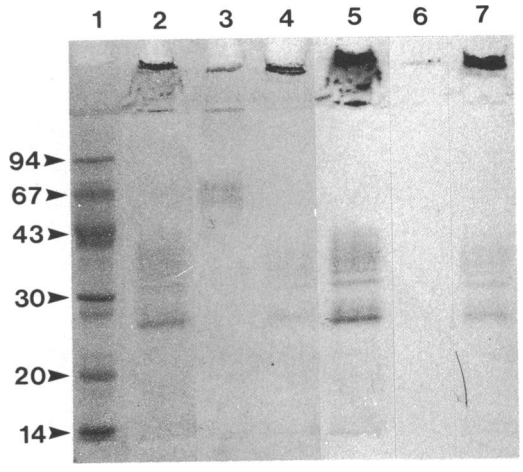

FIG. 1. Coomassie brilliant blue R-250-stained SDS-polyacrylamide gel containing a Bio-Rad low-molecular-weight standard (lane 1), SDS–β-ME–EDTA-solubilized ^{35}S-labeled sheath (lane 2) (see reference 25), a PS fraction from a ^{35}S-labeled sheath (lane 3), and the remaining PI material after the phenol extraction (lane 4) (see reference 26 for more details) and an autoradiogram of lanes 2, 3, and 4 in lanes 5, 6, and 7, respectively. Note the association of ^{35}S with all of the SDS–β-ME–EDTA-solubilized sheath proteins and all of the SDS–β-ME–EDTA-solubilized PI sheath proteins.

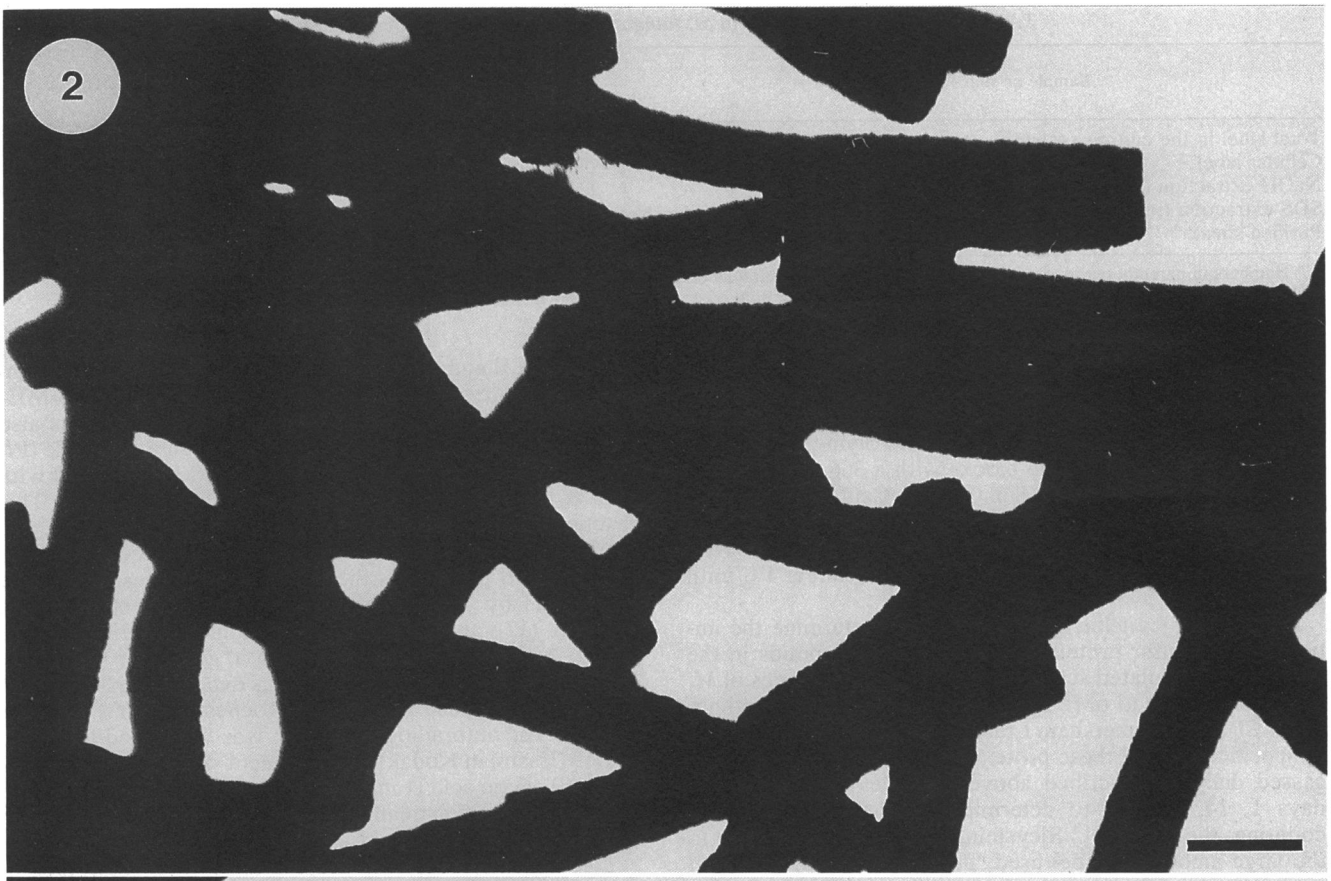
2

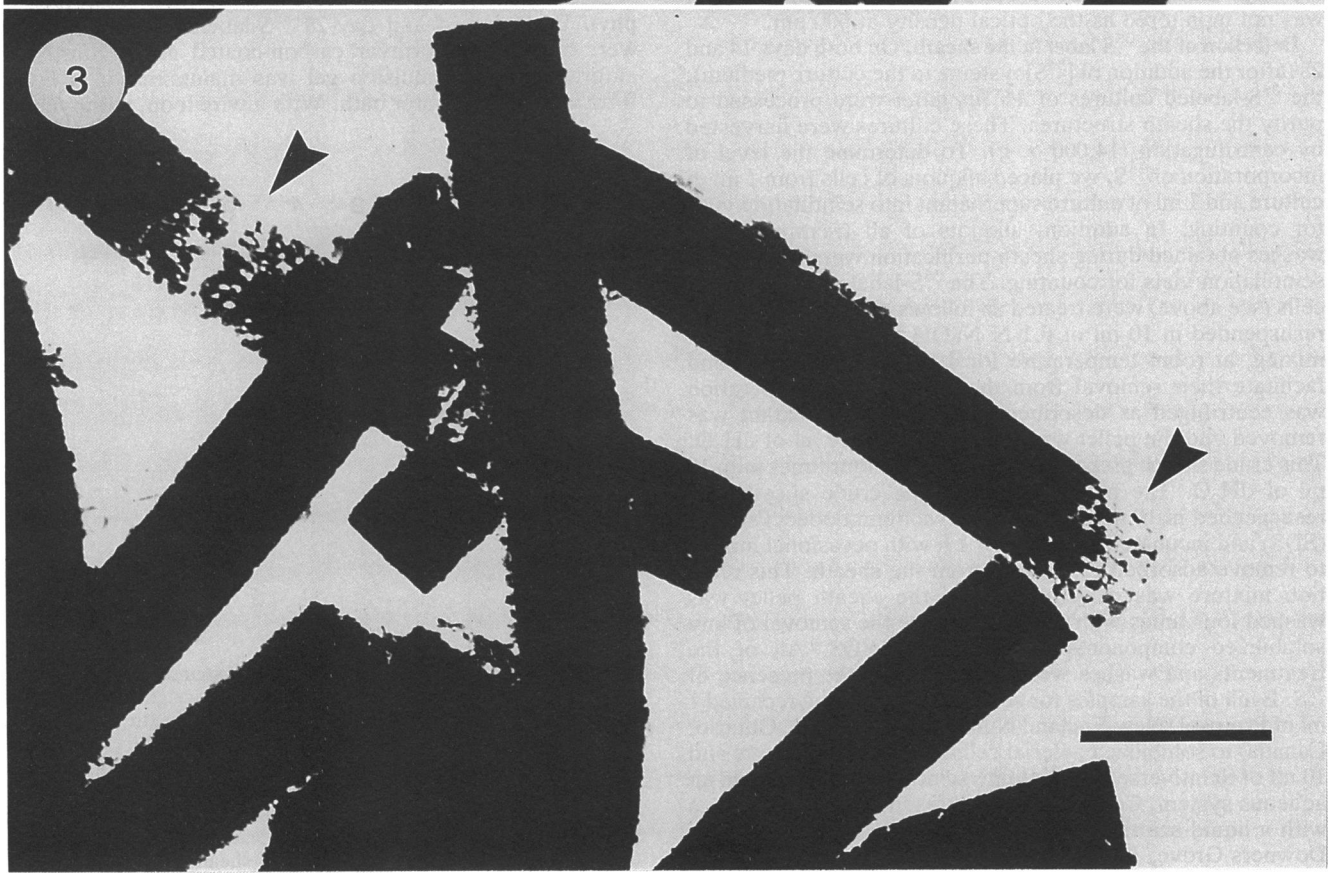
3

the autoradiographic emulsion was prepared so that the film was clear upon drying. This thin film was applied to a grid by passing the loop over a grid held with forceps. These sample-emulsion preparations were allowed to incubate for up to 1 week in a light-tight moisturized box and were developed as follows. The grids were incubated in D19 for 2 min, the reaction was stopped for 30 s with 2% (vol/vol) acetic acid, and the grids were fixed for 5 min in Ilford film fixer. The grids were washed with dH_2O for 30 min, air dried, and examined by transmission electron microscopy.

Preparation of spacer plugs and single-layer fragments of the sheath. A crude preparation of the *M. hungatei* sheath was obtained through spheroplast formation of cell cultures (26) and sucrose gradient centrifugation (27). This preparation was used to image spacer plugs by transmission electron microscopy with negative staining. Further purification of sheath material has been described (22). The purified sheath (5 ml of a 6.6-mg/ml solution) was passed through a French pressure cell (Amicon) at 124 kPa. The shear produced by this treatment fractured the sheath and allowed the examination of single, flattened fragments by transmission electron microscopy with negative staining.

Azo-mercurial labeling of exposed sulfhydryl groups. The purified *M. hungatei* sheath (1 ml of a 6-mg/ml solution) was reacted in SDS–β-ME–EDTA (22) at 100°C for 30 min to produce hoops. This preparation was centrifuged at 50,000 × *g* for 30 min. The pellet was washed once with dH_2O and finally resuspended in dH_2O to a final concentration of 6 mg/ml. To ensure the presence of hoops, we examined the preparation by transmission electron microscopy with and without the use of 2% (wt/vol) uranyl acetate as a negative stain to contrast the hoops.

Labeling of the sulfhydryl groups involved the suspension of 2.5 mg of the hoop preparation in 48 ml of heptanol (Eastman Kodak)-saturated (approximately 1.5 ml) 0.1 M glycine buffer in a 125-ml flask. Three milliliters of heptanol containing 6 μM 4-(*p*-dimethylaminobenzene-azo)phenylmercuric acetate (an azo-mercurial dye) (Sigma Chemical Co., St. Louis, Mo.) was immediately added (11). This reaction mixture was placed on a magnetic stir plate and stirred to enhance the surface interface chemistry between the two phases (the hoop suspension in glycine buffer and the heptanol-dye solution). The top of the flask was covered with Parafilm to reduce solvent evaporation, and the reaction was allowed to proceed for 24 h at room temperature. The progress of the experiment was monitored as a decrease in the A_{414} for the heptanol-dye mixture and a corresponding increase in the A_{460} for the glycine buffer-hoop fraction (3). The decrease and the increase were monitored at the maximum absorbance for unbound dye (A_{414}) and bound dye (A_{460}), respectively. After labeling for sulfhydryl groups with the azo-mercurial dye was done, the treated hoop preparation (Hg-hoops) was examined by transmission electron microscopy both with and without the use of 2% (wt/vol) uranyl acetate as a negative stain. The Hg-hoops were also examined for the presence of sulfur and mercury with a Philips EM400T electron microscope equipped with a LINK X-ray microanalyzer for electron-dispersive X-ray spectroscopy (EDS).

Hybridoma production and selection. Hybridomas were produced by the method of Oi and Herzenberg (14) as modified by Lane (13). The purified sheath was used as an antigen for the production and selection of MAbs specific for sheath polypeptides. The details of the procedure were described previously (22).

Colloidal gold labeling. Thin sections of Lowicryl K4M resin-embedded *M. hungatei* were probed with MAbs specific for SDS–β-ME–EDTA-soluble polypeptides (22) and for PS polypeptides (23). The adsorbed MAbs were then labeled with protein A-colloidal gold. All incubations were performed at room temperature and in high humidity to prevent dehydration of the reaction system. Lowicryl K4M resin sections were blocked with 1% (wt/vol) bovine serum albumin (BSA) in 0.01 M phosphate-buffered 0.14 M saline containing 0.1% (vol/vol) Tween 20, 0.1% (wt/vol) BSA, and 0.1% (wt/vol) sodium azide (PBS-TBA) for 30 min, after which the grids were washed with 10 ml of PBS-TBA applied dropwise. The grids were then placed on a 50-μl drop of hybridoma culture supernatant (MAb) for 1 h. Twenty milliliters of PBS-TBA was used to wash the grids (as described above) after MAb probing. The protein A-colloidal gold (3 μl) used in each labeling system represented a 1/20 dilution (in PBS/TBA) of stock colloidal gold prepared by the method of Frens (7) with the modifications of Bendayan (1) and Hicks and Molday (10). The grids were floated on this diluted gold sol for 1 h and washed as described for the MAb step. Prior to examination by transmission electron microscopy, the grids were washed dropwise with 10 ml of dH_2O and stained with 2% (wt/vol) uranyl acetate for 5 min.

Plasmolysis of *M. hungatei*. Sucrose was added under anaerobic conditions to a 10-ml exponential-phase culture of *M. hungatei* until a final concentration of 30% (wt/vol) was attained. Samples (1.5 ml) were removed at time zero (0 min) (just prior to the addition of sucrose, which dissolved within 30 s) and at 10, 20, and 30 min after sucrose addition. These samples were centrifuged at 14,000 × *g* for 1 min and resuspended in 4% (vol/vol) glutaraldehyde for 1 h at room temperature. The samples were then enrobed, processed through an ethanol-propylene oxide dehydration series, and embedded in Epon 812 for transmission electron microscopy.

RESULTS

Identification of sulfur proteins in the sheath. The growth of *M. hungatei* in the presence of [^{35}S]cysteine resulted in increased uptake of the radiolabel over time, with 0.67% efficiency at day 1 (data not shown), 5.65% efficiency at day 14 (Table 1), and 12.17% efficiency at day 28 (Table 1). Purification of the sheath from these radiolabeled cultures demonstrated that 8.48% (day 14) and 9.36% (day 28) of the total cellular sulfur was localized to this structure (Table 1). In Table 1, the percentage of label in the sheath refers to the amount of ^{35}S associated with the final sheath fraction in relation to the amount of cellular label present in intact cells. SDS-PAGE and autoradiography demonstrated that all of the SDS–β-ME–EDTA-solubilized sheath components contained ^{35}S, while PS polypeptides did not (Fig. 1).

FIG. 2. Thin-film EM autoradiogram of sheaths purified from a culture of *M. hungatei* grown in the presence of [^{35}S]cysteine for 14 days. Note the ^{35}S-mediated silver precipitation (black regions) that highlight the entire sheath structure. Bar, 1.0 μm.

FIG. 3. Thin-film EM autoradiogram of sheaths purified from a culture of *M. hungatei* grown in the presence of [^{35}S]cysteine for 28 days. Note the nonradiolabeled regions (arrowheads) of sheaths that were presumably associated with sites of cell division (i.e., new cell spacer regions within a filament) and with new cell poles (ends of the filaments). Bar, 1.0 μm.

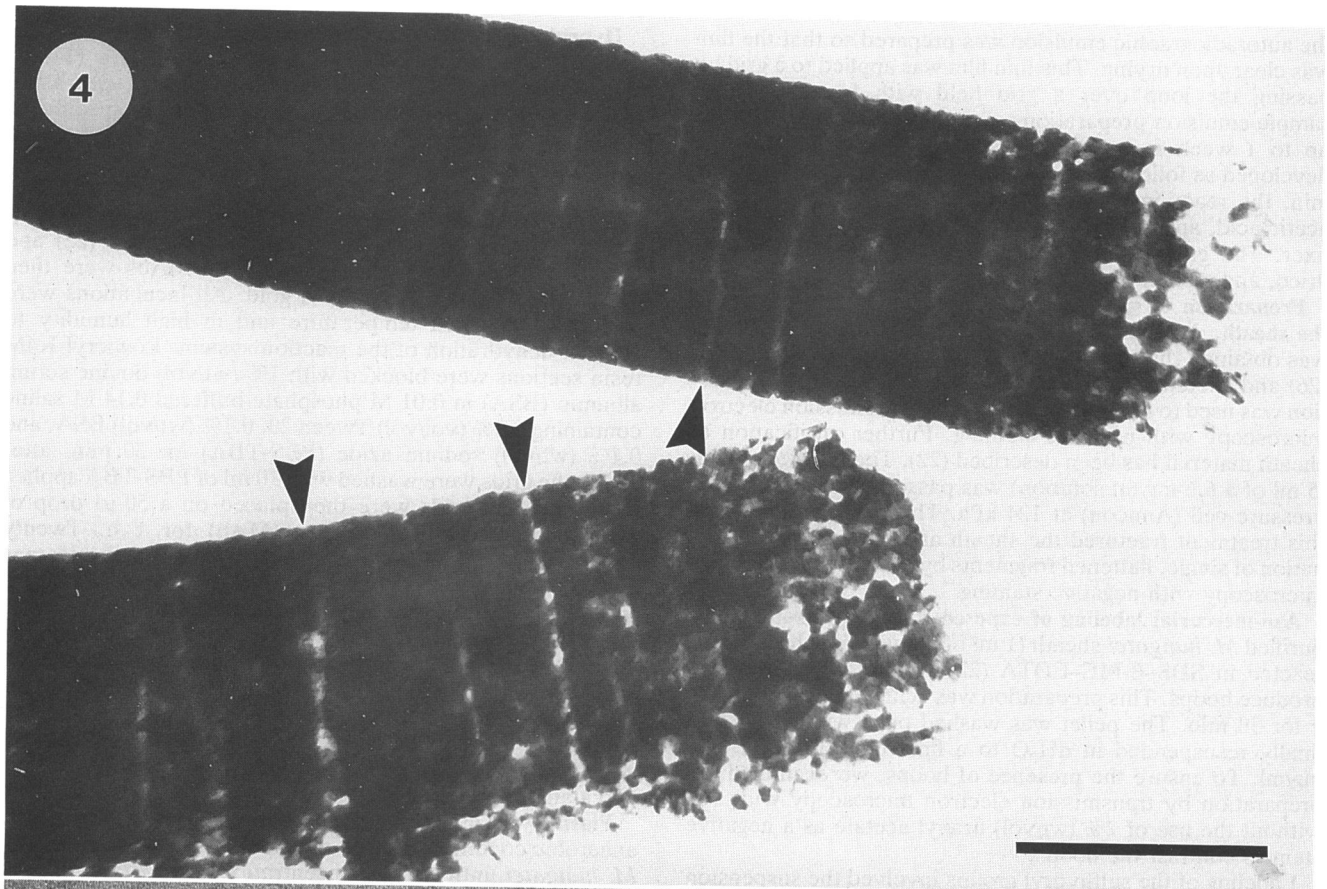
4

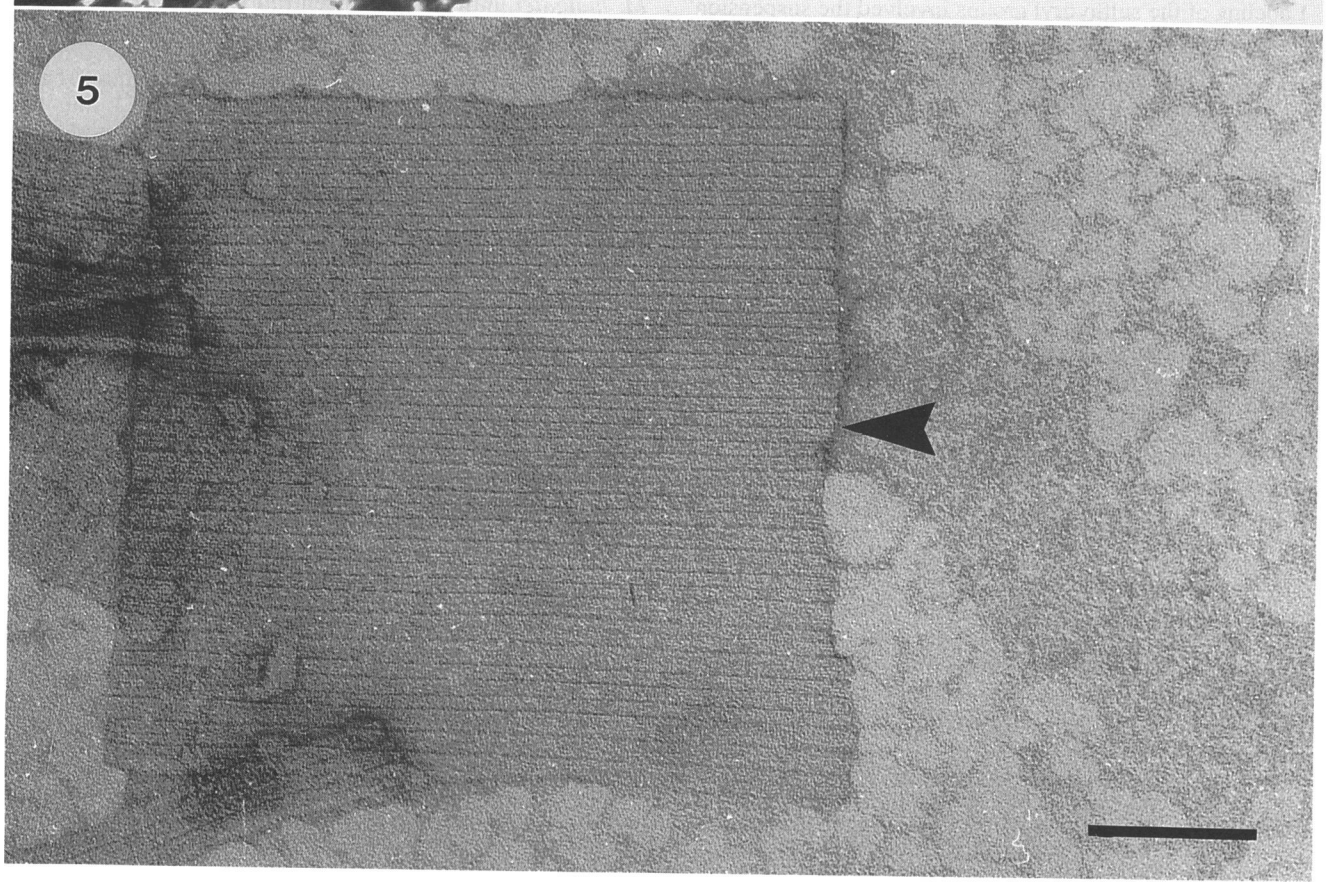
5

TABLE 2. Range in hoop widths and frequency in sheath tubes passed through a French pressure cell at 124 kPa

Width of hoops, expressed as no. of 2.8-nm repeats[a]	No. of hoops observed[a]	% of sheath tube length[b]
3	12	12.2
4	23	31.2
5	14	23.7
6	5	10.2
7	6	14.2
8	2	5.4
9	1	3.1

[a] Determined by counting the number of 2.8-nm repeats associated with each hoop in five micrographs of sheared sheaths (see, e.g., Fig. 5). The total analysis involved 827 nm of sheath along the longitudinal axis.
[b] Based on the total length of sheath that was analyzed.

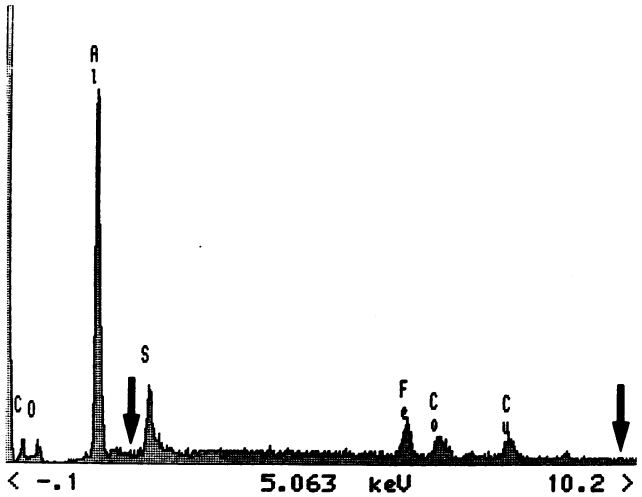

FIG. 6. EDS scan produced from either unlabeled hoops or Hg-hoops. No mercury peaks (arrows) were measured for the Hg-labeled hoop fraction. Note the presence of a sulfur peak associated with the Hg-labeled hoop fraction. The Fe, Cu, and Co peaks were derived from the specimen holder.

Sheath growth patterns revealed by sulfur incorporation. EM autoradiography of a day-14 radiolabeled sheath revealed that the ^{35}S was incorporated throughout the structure (Fig. 2). This result was evident by the photoreduction of silver by the radiolabel (black regions) in the characteristic, rectangularly shaped collapsed sheath tubes with dimensions of ≈0.67 μm by tens of micrometers. A similar examination of a day-28 ^{35}S-labeled sheath demonstrated that although ^{35}S was detected throughout most of the sheath, clearing zones in the autoradiogram that corresponded to the presence of nonradiolabeled sulfur in specific regions of the sheath also occurred. These clearing zones typically occurred at approximately one cell length (~8 μm) from the ends of sheath tubes (Fig. 3). Incorporation of new sheath constituents (including organosulfur compounds) in these regions likely corresponds to division sites in the original filament before sheath purification. Other, less obvious (narrow) regions of nonradioactive sulfur were located along the lengths of the sheath tubes (Fig. 4). In this sense, the chase was done with cold cysteine, and the question is simply why hot cysteine was not incorporated if it was available.

Hoop development (growth) was evident through the examination of sheaths that had been sheared by use of a French pressure cell. Negative staining demonstrated that hoops contained from three to nine rows of 2.8-nm lattice particle repeats along their widths. A summary of hoop widths, occurrence, and percentage of the tube length is presented in Table 2. The range in hoop widths suggests that hoop growth and division occur along the length of the sheath tube, the wide hoops (i.e., those with more particle repeats) being older hoops that are close to division and the narrow hoops (i.e., those with few particle repeats) being younger hoops that have recently split.

Occurrence of exposed sulfhydryl groups. Spectrophotometric analysis revealed that hoops became labeled with the azo-mercurial dye (Hg-hoops). The A_{414} of the heptanol-dye system decreased (−0.440), while the A_{460} of the aqueous hoop system increased (0.194). Hg-hoops (i.e., hoops with Hg bound to sulfhydryl groups) were found to be more electron dense than the starting hoop material by transmission electron microscopy. However, the labeling was diffuse, and no distinct (periodic) labeling pattern on the Hg-hoops was evident (data not shown). In negative stains, the 2.8-nm repeats (Fig. 5) could be seen, demonstrating that the heptanol-dye mixture did not cause structural alterations of the hoops (data not shown). The concentration of Hg in the Hg-hoops was below the levels detectable by EDS, which provides an elemental analysis, although sulfur was easily identifiable (Fig. 6). Therefore, only a limited number of exposed sulfhydryl sites (as opposed to total sulfur) were available for interaction with the azo-mercurial dye.

Colloidal gold labeling. To gain more information about sheath growth, we localized sheath proteins by antibody–protein A-colloidal gold labeling of thin sections of Lowicryl K4M resin-embedded intact cells of *M. hungatei*. The immunological probes specific for the SDS–β-ME–EDTA-solubilized proteins and for the PS proteins were localized to the sheath, plasma membrane, cell spacer region, and internal sites (Fig. 7 and 8). All of the immunological probes demonstrated a degree of labeling well above that of the background (Table 3).

Additional cell envelope structures. On the basis of measurements between the ends of the radiolabeled sheath tubes and the clearing zones (Fig. 3), EM autoradiography highlighted the cell spacer region of *M. hungatei* as the most active region of growth for this organism. Examination of

FIG. 4. Underexposed thin-film EM autoradiogram of sheaths purified from a culture of *M. hungatei* grown in the presence of [^{35}S]cysteine for 28 days. This micrograph was purposely underexposed to emphasize the incorporation of nonradioactive sulfur at discrete hoop-like regions along the lengths of the sheath tubes (arrowheads). Negative staining of analogous whole mounts of sheaths confirmed that there was no actual (physical) separation between the hoops and that the sheaths were intact. Bar, 0.5 μm.

FIG. 5. Electron micrograph of a sheared sheath negatively stained with 2% (wt/vol) uranyl acetate. The hoop boundaries are more intensely stained (along the direction of the arrowhead) than are the 2.8-nm periodic units within the hoops. Sheared sheaths typically break in nearly straight lines, both along hoop boundaries and longitudinally across adjoining hoops. Differences in hoop widths can easily be seen by aligning your eye to the edge of the page along the hoop axis. Bar, 100 nm.

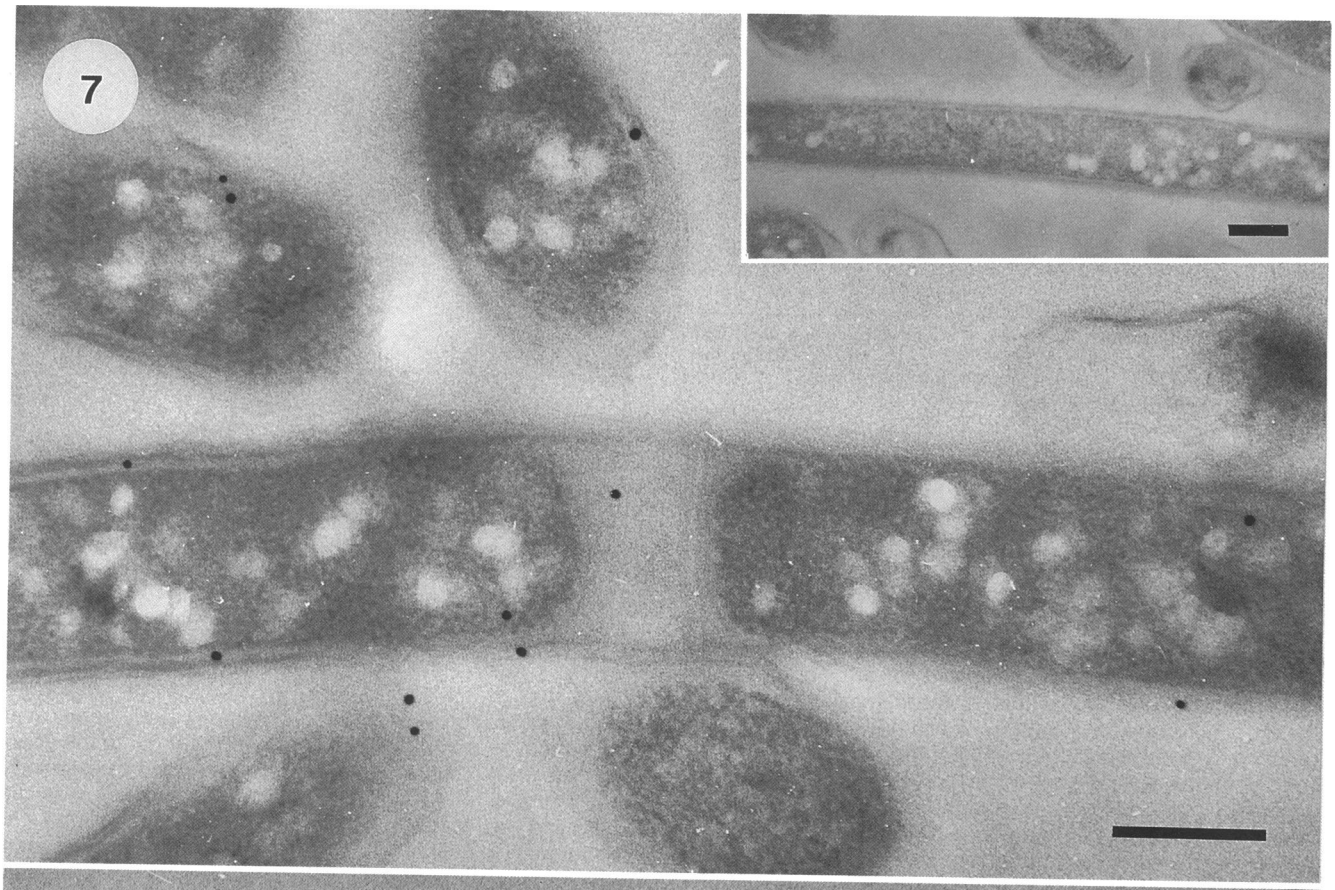
7

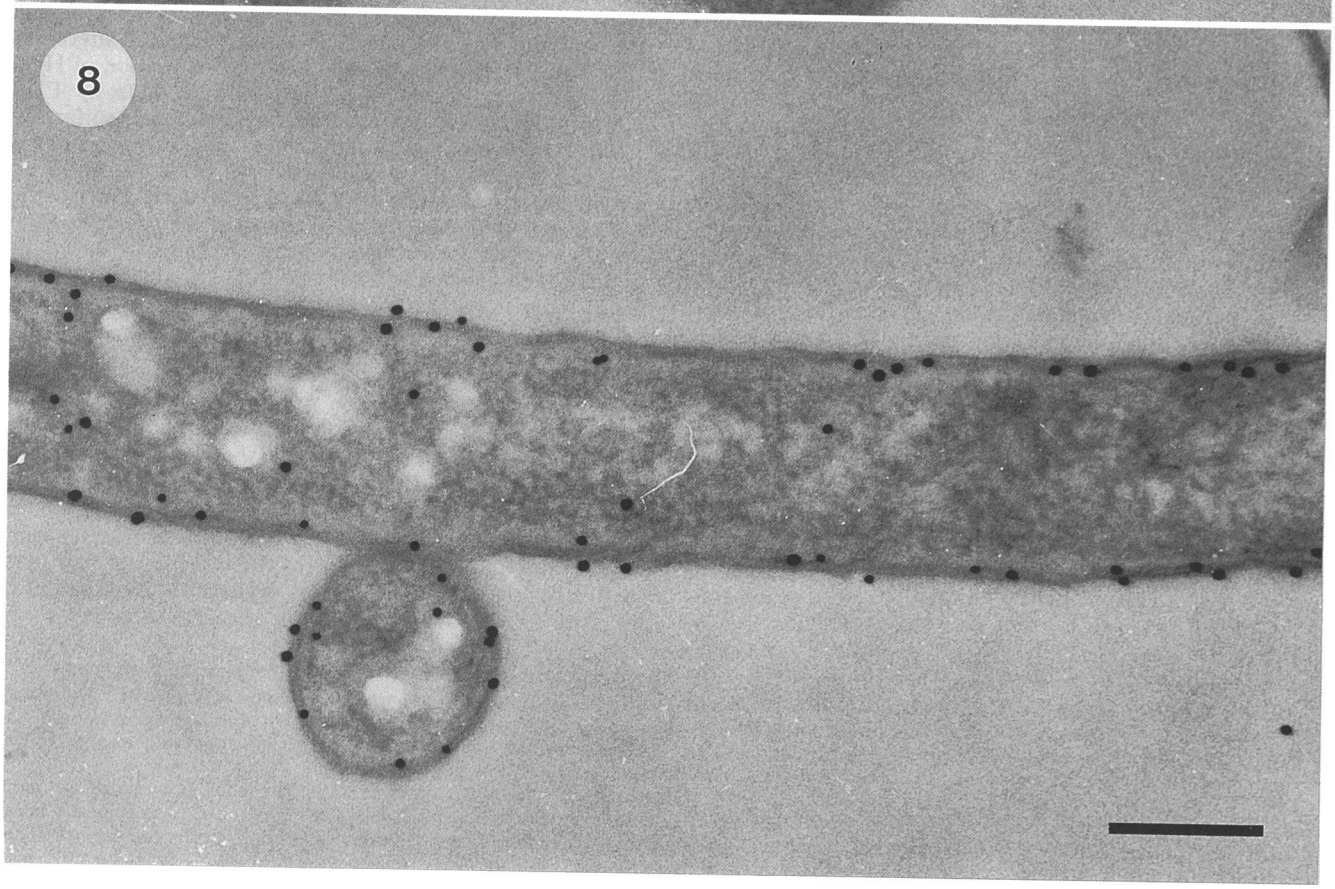
8

TABLE 3. Distribution of colloidal gold in Lowicryl K4M resin sections[a]

MAb probe	Distribution (counts) of colloidal gold in:				Background counts	Cell label[c] counts	Ratio[d]
	Sheath	Plasma membrane	Spacer region	Internal sites[b]			
1.8[e]	178	91	28	75	6	372	120:1
19.1[e]	621	229	39	204	42	1,093	104:1
20.7[e]	273	119	42	183	19	617	71:1
25.1[f]	39	13	19	11	4	82	34:1
26.1[f]	250	57	5	5	22	317	35:1
None (control)	2	1	0	4	25	7	1:1

[a] Regions of ~100 μm^2 were examined for each labeling study (ca. one-third of this surface area was occupied by sectioned bacteria.
[b] Cytoplasmic.
[c] In sheath, plasma membrane, spacer region, and internal sites.
[d] Ratio of cell label counts to background counts after the cell label was adjusted to represent a proportionate surface area.
[e] Specific for PS constituents.
[f] Specific for SDS–β-ME–EDTA-soluble constituents.

this spacer region in a thin section by transmission electron microscopy (Fig. 9) revealed a complex multilayered architecture (sheath, spacer plugs, cell spacer, cell wall, plasma membrane, and cytoplasm) that has been described in previous studies (2, 5, 6, 20). Plasmolysis did not separate the protoplast from the cell wall but deformed both the cell wall and the plasma membrane (Fig. 10). With this deformation, both structures were separated from the sheath and a previously unseen periodicity in the cell wall was revealed. The cell wall, like the sheath, could be paracrystalline in structure but with larger subunit spacings. A spacer plug trapped within a collapsed sheath cylinder (Fig. 11) demonstrated the paracrystalline nature of the spacer plugs. The cell envelope of *M. hungatei* appears to consist of three paracrystalline assemblies: the cell wall, the spacer plugs, and the sheath.

DISCUSSION

Our initial goal in this study was to examine not only the occurrence of organosulfur in the sheath of *M. hungatei* (Table 1) but also its molecular association. The detection of S by EDS and the detection of the presence of approximately 9% of the cellular sulfur in the proteinaceous sheath (of cultures grown with [^{35}S]cysteine) indicate that sulfer containing regions exist, and it is likely that disulfide bonds (cystine) contribute to the resilience of the sheath (6).

The initial step towards the incorporation of new constituents into a preexisting sheath and concomitant sheath growth (an indicator of bacterial growth) is the cytoplasm- or membrane-mediated synthesis of new protein. Protein A-colloidal gold-immunolabeled thin sections of *M. hungatei* (Fig. 7 and 8) showed the presence of sheath proteins in the cytoplasm, suggesting that these proteins are synthesized in the cytoplasm and that posttranslational translocation (30) may be used for the transfer of these proteins across the plasma membrane. The SDS–β-ME–EDTA-soluble polypeptides were best labeled by ^{35}S, and it is presumably these that we first saw synthesized in the cytoplasm. They represent ~70% of the mass of the sheath (22) and are responsible for the 2.8-nm repeats (23, 29).

Sheath growth requires efficient transport (likely diffusion) of sheath precursors across the cell wall to the preexisting sheath and to the inner surface of the spacer plugs (Fig. 9). Since enhanced growth was observed in the cell spacer region and not along the cylindrical portion adjacent to the bacterium, *M. hungatei* must possess some mechanism (24) of exporting and concentrating sheath precursors in this region. Unlike other S-layer systems that depend on relatively weak bonds to anneal their self-assembled subunits together, the sheath depends on strong covalent bonds. Although self-promoted covalent bonding is possible if select reactive chemical sites are energetically primed, most biological systems rely on enzyme catalysis. At present, we have no information on how this covalent bonding proceeds, but either mechanism would represent a novel mechanism of S-layer assembly. Conceptually, the supply of sheath precursors for growth in cell spacer regions can rely on diffusion through pores (ca. 15 nm [20]) in spacer plugs (Fig. 11). As the cell spacer regions enlarge (sheath growth), the sheath precursors are continually used up and the "empty" volume increases. Therefore, the incorporation of sheath precursors in cell spacer regions would have a synergistic effect in producing the diffusion gradient necessary for the transport of sheath precursors into cell spacer regions.

We are not aware of any other studies on the growth of prokaryotic sheath structures, and we must rely on information obtained from studies on other bacterial S-layer systems. In general, S-layer growth patterns are controlled by sliding dislocations that serve as insertion sites for new material (9, 19, 21). The importance of the paracrystalline structure of S layers and of sliding dislocations in cell growth was outlined by Gruber and Sleytr (8), who demonstrated that the hexagonally ordered S layer of *Bacillus stearothermophilis* PV 72 was incorporated in a helical manner corresponding to the angle of symmetry of the pattern. The necessity of crystal discontinuities for the incorporation of

FIG. 7. Thin section of Lowicryl K4M resin-embedded *M. hungatei* probed with MAb 25.1 (which is specific for SDS–β-ME–EDTA-soluble constituents) and protein A-colloidal gold. Note the occurrence of colloidal gold on the sheath, at internal sites, and in the cell spacer region. (Inset) Thin section of Lowicryl K4M resin-embedded *M. hungatei* probed only with protein A-colloidal gold and no antibody to serve as a control. The low degree of labeling suggests that blocking with BSA is sufficient to inhibit most nonspecific binding of protein A-colloidal gold. Bars, 0.5 μm.

FIG. 8. Thin section of Lowicryl K4M resin-embedded *M. hungatei* probed with MAb 19.1 (which is specific for PS constituents) and protein A-colloidal gold. Note the labeling of the sheath, plasma membrane, and internal sites. Bar, 0.5 μm.

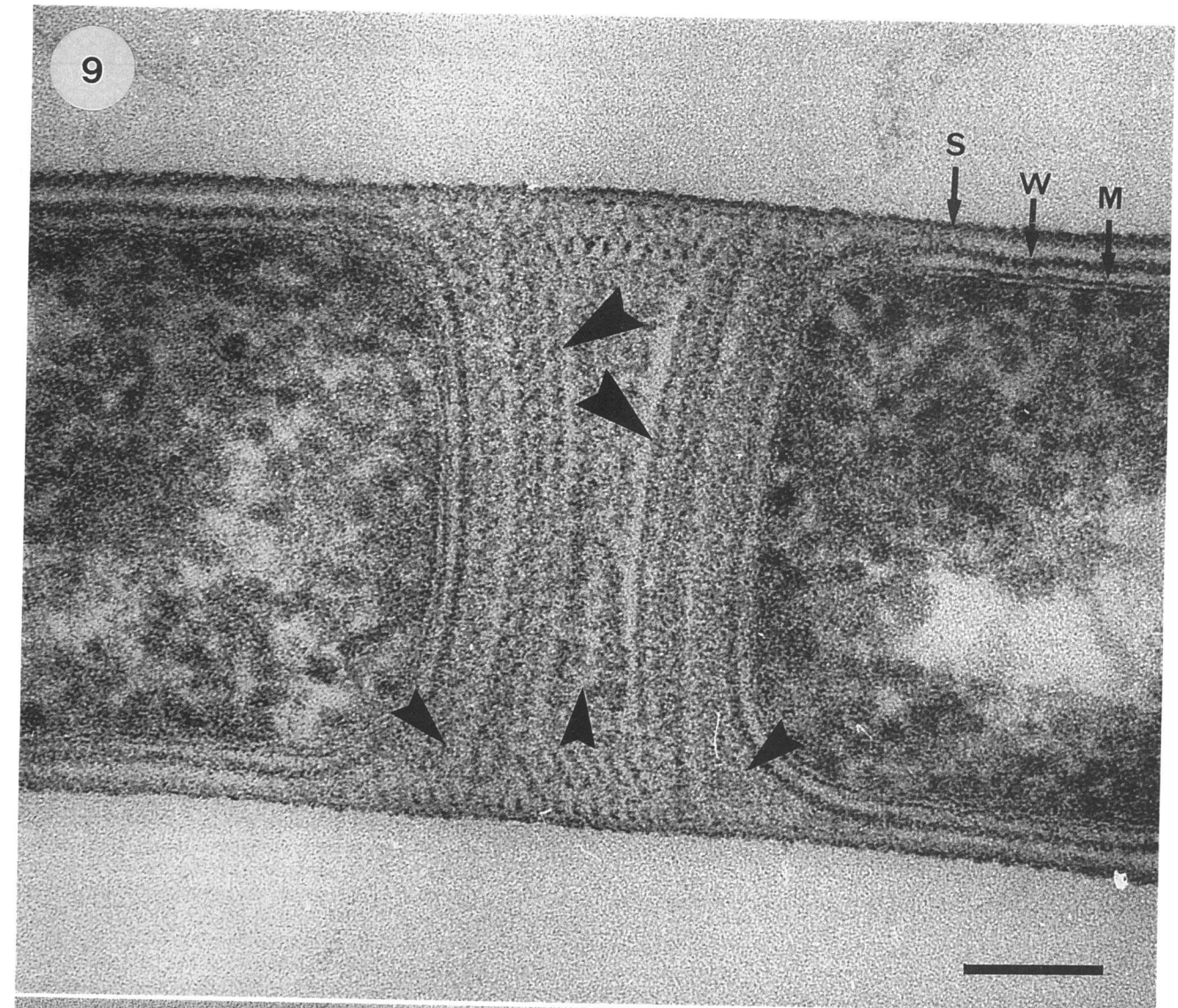
9
S
W
M

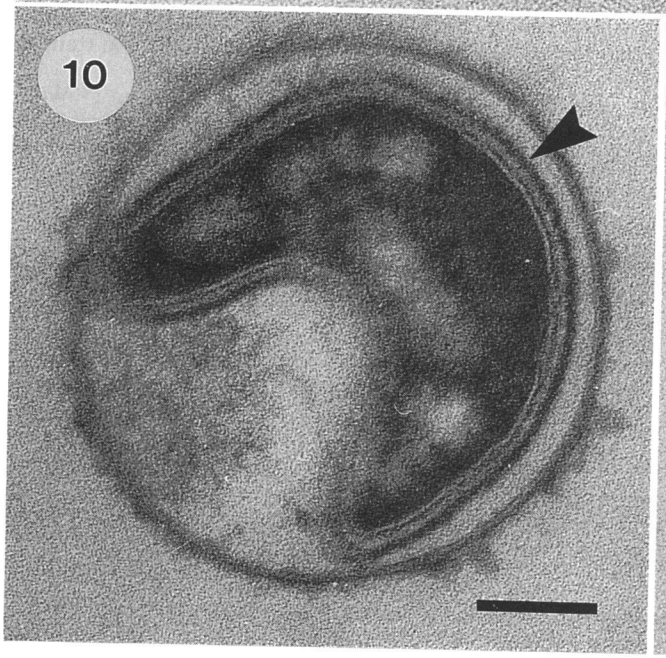
10

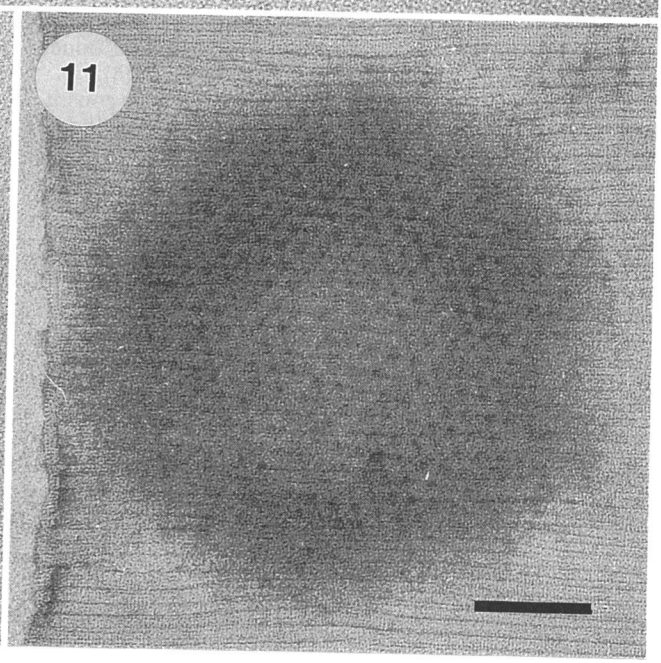
11

FIG. 9. Thin section of *M. hungatei*. Note the sheath structure (S), cell wall (W), plasma membrane (M), and multilayered spacer plugs (large arrowheads). Also note the amorphous material between the cell wall and the spacer plug and within the cell spacer region (small arrowheads). Bar, 100 nm.

FIG. 10. Cross section of *M. hungatei* plasmolysed with 30% sucrose for 10 min. Note the periodicity of the cell wall (arrowhead). Bar, 100 nm.

FIG. 11. Negative stain (2% [wt/vol] uranyl acetate) of part of a sheath containing a disc-shaped plug. Note the hexagonal symmetry in the plug (for more detailed information, see reference 5) and the paracrystalline nature of the sheath (for more detailed information, see reference 29). Bar, 100 nm.

the S layer and concomitant cell growth is particularly apparent in the recent study by Pum et al. (19) of *Methanocorpusculum sinense*, which possesses only an S layer as its wall. Controlled cleavage of the subunits in the existing pattern and insertion of newly synthesized subunits in the existing pattern are required to accommodate growth and to prevent destruction of the protoplast because of cellular turgor pressure. In *M. sinense*, these processes are accomplished with multiple, sliding dislocation cores that consist of fivefold and sevenfold rings and that produce wedge dislocations at sites of insertion of new S-layer material. In *M. hungatei*, the narrow zones of growth along the cylindrical region of the cells (Fig. 4) can only correspond to the de novo development of hoops. Because of the paracrystalline nature of the sheath, both growth regions (i.e., the cylindrical regions close to cells and the cell spacer regions; Fig. 3 and 4) must rely on the incorporation of new material (into hoops) so that the hoops become wider and wider until they eventually split in two. Narrower hoops (i.e., those with three or four 2.8-nm repeats [Table 2]) are, therefore, recently split hoops and are the youngest hoops, whereas wider hoops (i.e., those with six to nine 2.8-nm repeats [Table 2]) are ready to split and are the oldest hoops. Actively growing regions of the sheath (the cell spacer regions) would likely have the highest frequency of narrow (young) and wide (old) hoops but, so far, we do not have the ability to detect this possibility.

The sheath in *M. hungatei* is also a stress-bearing structure (2, 28), and new material must be inserted without the release of turgor pressure, or cell lysis will ensue. Perhaps this is the prime reason why most sheath assembly occurs far removed from cells, at the cell spacer regions.

At the macromolecular level, the sulfur proteins have been localized by colloidal gold immunoprobes to both the inner and the outer surfaces of the sheath (22). During sheath growth, the transfer of these polypeptides from the inner to the outer surface of the sheath (maturation; 4) must occur without the perturbation of the stress-bearing capacity of the sheath. The rigidity imparted by the PS proteins (23) may help stabilize the sulfur proteins during (or after) maturation. Because the outer circumference is slightly larger than the inner circumference and because new material must be incorporated at the inner sheath face, *M. hungatei* must possess a mechanism to decrease the number of stress-bearing bonds at the outer surface. The partial degradation of an intact sheath into hoops by treatment with β-ME, a disulfide bond breaker, implicates sulfur-sulfur bonding in sheath stability and, quite possibly, in the formation of the 2.8-nm paracrystalline repeats of the sheath. The breakage of specific disulfide bonds at the outer sheath face would (i) function as a stress-releasing mechanism to accommodate sheath growth and (ii) result in the separation of amorphous material into regularly arrayed particles (2.8 nm). The limited surface exposure of sulfhydryl groups on hoops (azomercurial labeling study) supports the internalization of most of the sulfur constituents. Alternatively, the cystine linkages could act as hinge regions, resulting in grooves between the constituent hoops (Fig. 5). These grooves (hoop boundaries) therefore would be a purely physical phenomenon resulting from cell turgor. This is the first bacterial S layer to be characterized with sufficient quantities of sulfur to imply the possible involvement of cystine in its structural integrity (Fig. 3). Conceptually, the cystine constituents could function in chemical stability through covalent bonding and as selective cleavage sites (or hinge regions) to release stress to accommodate growth.

ACKNOWLEDGMENTS

G.S. was supported by a Natural Sciences and Engineering Research Council of Canada graduate student fellowship during this study. The actual research was supported by an operating grant from the Medical Research Council of Canada to T.J.B., and the electron microscopy was performed in the NSERC Guelph Regional Facility, which is partially supported by a Natural Sciences and Engineering Research Council of Canada infrastructure grant.

Advice from G. D. Sprott, Division of Biological Sciences, National Research Council of Canada, was greatly appreciated. Special thanks are due to C. MacKenzie for word processing.

REFERENCES

1. **Bendayan, M.** 1982. Double immunocytochemical labelling applying the protein A-gold technique. J. Histochem. Cytochem. **30**:81–85.
2. **Beveridge, T. J., B. J. Harris, and G. D. Sprott.** 1987. Septation and filament splitting in *Methanospirillum hungatei*. Can. J. Microbiol. **33**:725–732.
3. **Beveridge, T. J., and R. G. E. Murray.** 1980. Sites of metal deposition in the cell wall of *Bacillus subtilis*. J. Bacteriol. **141**:876–887.
4. **Beveridge, T. J., G. Southam, M. H. Jericho, and B. L. Blackford.** 1990. High-resolution topography of the S-layer sheath of the archaebacterium *Methanospirillum hungatei* provided by scanning tunneling microscopy. J. Bacteriol. **172**:6589–6595.
5. **Beveridge, T. J., G. D. Sprott, and P. Whippey.** 1991. Ultrastructure, inferred porosity, and Gram-staining character of *Methanospirillum hungatei* filament termini describe a unique cell permeability for this archaeobacterium. J. Bacteriol. **173**: 130–140.
6. **Beveridge, T. J., M. Stewart, R. J. Doyle, and G. D. Sprott.** 1985. Unusual stability of the *Methanospirillum hungatei* sheath. J. Bacteriol. **162**:728–737.
7. **Frens, G.** 1973. Controlled nucleation for the regulation of particle size in monodisperse gold suspensions. Nature (London) Phys. Sci. **241**:20–22.
8. **Gruber, K., and U. B. Sleytr.** 1988. Localized insertion of new S-layer during growth of *Bacillus stearothermophilis* strains. Arch. Microbiol. **149**:485–491.
9. **Harris, W. F., and L. E. Scriven.** 1970. Functions of dislocation in cell walls and membranes. Nature (London) **228**:827–829.
10. **Hicks, D., and R. S. Molday.** 1984. Analysis of cell labelling for scanning and transmission electron microscopy, p. 203–219. *In* J. P. Revel, T. Barnard, and G. H. Haggis (ed.), The science of biological specimen preparation for microscopy and microanal-

ysis. Scanning Microscopy International, Chicago.
11. **Horowitz, M. G., and I. M. Klotz.** 1956. Interaction of an azomercurial with proteins. Arch. Biochem. Biophys. **63:**77–86.
12. **Laemmli, U. K.** 1970. Cleavage of structural proteins during the assembly of the head of bacteriophage T4. Nature (London) **127:**680–685.
13. **Lane, R. D.** 1985. A short duration polyethylene glycol fusion technique for increasing production of monoclonal antibody-secreting hybridomas. J. Immunol. Methods **81:**223–228.
14. **Oi, V. T., and L. A. Herzenberg.** 1979. Immunoglobulin producing hybrid cell lines, p. 351–371. *In* B. B. Mishell and S. M. Shiigi (ed.), Selected methods in cellular immunology. W. H. Freeman & Co., San Francisco.
15. **Patel, G. B., A. W. Kahn, and L. A. Roth.** 1978. Optimum levels of sulphate and iron for the cultivation of pure cultures of methanogens in synthetic media. J. Appl. Bacteriol. **45:**347–356.
16. **Patel, G. B., L. A. Roth, and G. D. Sprott.** 1979. Factors influencing filament length of *Methanospirillum hungatii*. J. Gen. Microbiol. **112:**411–415.
17. **Patel, G. B., L. A. Roth, L. van den Berg, and D. S. Clark.** 1976. Characterization of a strain of *Methanospirillum hungatii*. Can. J. Microbiol. **22:**1404–1410.
18. **Patel, G. B., G. D. Sprott, R. W. Humphrey, and T. J. Beveridge.** 1986. Comparative analysis of the sheath structures of *Methanothrix concilii* GP6 and *Methanospirillum hungatei* strains GP1 and JF1. Can. J. Microbiol. **32:**623–631.
19. **Pum, D., P. Messner, and U. B. Sleytr.** 1991. Role of the S layer in morphogenesis and cell division of the archaebacterium *Methanocorpusculum sinense*. J. Bacteriol. **173:**6865–6873.
20. **Shaw, P. J., G. J. Hills, J. A. Henwood, J. E. Harris, and D. B. Archer.** 1985. Three-dimensional architecture of the cell sheath and septa of *Methanospirillum hungatei*. J. Bacteriol. **161:**750–757.
21. **Sleytr, U. B., and P. Messner.** 1988. Crystalline surface layers in prokaryotes. J. Bacteriol. **170:**2891–2897.
22. **Southam, G., and T. J. Beveridge.** 1991. Immunochemical analysis of the sheath of the archaeobacterium *Methanospirillum hungatei* GP1. J. Bacteriol. **173:**6213–6222.
23. **Southam, G., and T. J. Beveridge.** 1992. Characterization of a novel, phenol-soluble group of polypeptides which convey rigidity to the sheath of *Methanospirillum hungatei* GP1. J. Bacteriol. **174:**935–946.
24. **Southam, G., M. L. Kalmokoff, K. F. Jarrell, S. F. Koval, and T. J. Beveridge.** 1990. Isolation, characterization, and cellular insertion of the flagella from two strains of the archaebacterium *Methanospirillum hungatei*. J. Bacteriol. **172:**3221–3228.
25. **Sprott, G. D., T. J. Beveridge, G. B. Patel, and G. Ferrante.** 1986. Sheath disassembly in *Methanospirillum hungatei* strain GP1. Can. J. Microbiol. **32:**847–854.
26. **Sprott, G. D., J. R. Colvin, and R. C. McKellar.** 1979. Spheroplasts of *Methanospirillum hungatii* formed upon treatment with dithiothreitol. Can. J. Microbiol. **25:**730–738.
27. **Sprott, G. D., and R. C. McKellar.** 1980. Composition and properties of the cell wall of *Methanospirillum hungatei*. Can. J. Microbiol. **26:**115–120.
28. **Sprott, G. D., K. M. Shaw, and K. F. Jarrell.** 1983. Isolation and chemical composition of the cytoplasmic membrane of the archaebacterium *Methanospirillum hungatei*. J. Biol. Chem. **258:**4026–4031.
29. **Stewart, M., T. J. Beveridge, and G. D. Sprott.** 1985. Crystalline order to high resolution in the sheath of *Methanospirillum hungatei*: a cross-beta structure. J. Mol. Biol. **183:**509–515.
30. **Wickner, W., G. Mandel, C. Zwizinski, M. Bates, and T. Killick.** 1978. Synthesis of phage M13 coat protein and its assembly into membranes *in vitro*. Proc. Natl. Acad. Sci. USA **75:**1754–1758.